water

MDPI

Article

A New Perspective to Explore the Hydraulic Connectivity of Karst Aquifer System in Jinan Spring Catchment, China

Zhengxian Zhang [1], Weiping Wang [1,*], Shisong Qu [1], Qiang Huang [2], Shuai Liu [1], Qiaoyi Xu [2] and Ludong Ni [1]

[1] School of Water Conservancy and Environment, University of Jinan, Jinan 250022, China; ZZXSIN@126.com (Z.Z.); stu_quss@ujn.edu.cn (S.Q.); 15053130651@163.com (S.L.); nld19941121@126.com (L.N.)

[2] Jinan City Qingyuan Water Group Co. Ltd., Jinan 250022, China; huanghqyy@163.com (Q.H.); happyxuqiaoyi@126.com (Q.X.)

* Correspondence: stu_wangwp@ujn.edu.cn; Tel.: +86-139-5316-2318

Received: 15 August 2018; Accepted: 25 September 2018; Published: 30 September 2018

Abstract: Investigating the hydraulic connectivity of a complex karst aquifer system is an important research topic for sustainable operation and optimization layout of karst groundwater exploitation and recharge. However, the identification of preferential sites of recharge and exploitation is usually subject to regional hydrogeology conditions and the mechanisms of recharge and exploitation. The conventional research methods of hydraulic connectivity often have some limitations. In this study, we developed an improved grey amplitude relation model to explore the hydraulic connectivity in Jinan spring catchment and presented a quantized evaluation index water table fluctuation relation degree (WTFRD) using karst groundwater table data in Western Jinan and Jinan spring groups from 2014 to 2017. Results showed that the total WTFRD was 0.854 between Western Jinan and Jinan spring groups when the external distraction for karst groundwater table was the smallest, which was in high relation degree grade. Meanwhile, the change rules of karst groundwater table in the two sites were basically the same. Accordingly, a high connectivity occurred between the two karst aquifers from a statistical perspective, and further illustrated that Western Jinan could be selected as preferential experiment sites. A comprehensive case in Jinan spring catchment indicated that the WTFRD provided a preliminary idea to investigate hydraulic connectivity quantitatively. This method could be considered as a pre-study of the conventional experiments to form a high-efficiency and low-cost combined method, which has great potential and merits further study.

Keywords: hydraulic connectivity; improved grey amplitude relation model; quantized evaluation index; water table fluctuation relation degree; combined method

1. Introduction

Jinan is well-known for its springs and is known as "Spring City", and therefore attracts many tourists. The natural spring water resources have historically contributed to the socioeconomic development of Jinan. In recent years, the rapid urbanization process and the sharply increased urban population has resulted in huge pressure on the urban water supply and an increasingly prominent contradiction between supply and demand. This situation will raise the over-extraction of karst groundwater, which causes the karst groundwater table and the outflow of springs to be reduced considerably in Jinan spring groups. The drying-up phenomenon in springs has occurred many times, and the regional groundwater ecosystem has undergone a series of negative impacts. Moreover, considering the poor water infrastructure and the few sources of urban water supply in

Jinan, the government urgently requires measures to ensure abundant and sustainable water resources for spring water protection and urban daily use. Therefore, the surface water of the South–North Water Diversion Project and Yellow River has been gradually used by Jinan as urban water supply sources. Although these measures can relieve the pressure of urban water supply and reduce the exploitation of karst groundwater to a certain extent, they do not fundamentally repair the regional groundwater funnel caused by over-exploitation of groundwater. Hence, launching an effective groundwater recharge project to recover groundwater resources and maintain perennial outflow of the springs is necessary. However, the geological structure of Jinan is rather complex; blindly conducting the recharge project not only has a heavy workload but also causes a huge consumption of labor, material resources, finance, and water resources. Thus, selecting preferential sites to optimize the layout of recharge and exploitation following the hydraulic connectivity is a critical link in executing the projects for urban water supply and spring protection.

Traditional studies on the hydraulic connectivity of karst aquifers have been conducted by measurement of hydraulic head (pumping test), hydrochemistry ion and environmental isotope tracer tests, and numerical simulation [1–4]. These studies provide additional insights for exploring hydraulic connectivity and play an important role in environmental and hydraulic engineering. Other examples of studies that have adopted hydrochemistry ion and environmental isotope methods to explore long-term hydrogeological patterns and hydraulic connectivity were described in references [5–9]. Kattan [10] recently investigated the aquifer interaction and the origin of groundwater salinization using hydrochemical and environmental isotope methods based on the karst groundwater quality of wells in Syria. The author described the hydraulic connectivity in the Hongdunzi coal mining region in Northwest China by employing hydrochemical and environmental isotope methods [11]. The appeal of numerical simulation for exploring the hydraulic connectivity of karst aquifer systems is that it combines water flow models with computer science, thereby facilitating visualization of simulation results [12–15]. The effects of the aquifer connectivity and geological structure on groundwater flow were described by using FEFLOW software to build the 3D geological model [16]. Raiber [17] developed a multilayer 3D hydrogeology model that introduced long-term monitoring data to describe the hydraulic connection of the aquifer in Wairau Plain, New Zealand. The hydrogeological parameters over the past 35 years in the study area were carefully surveyed, and on this basis, the hydraulic connectivity in the unconfined aquifer was investigated by Visual MODFLOW software [18].

The multiple methods have been combined with one another, to try to draw on the advantages of different methods to investigate the connectivity and feature of a complex aquifer system [19–23]. Environmental isotope tracers and hydrochemistry ions, which flow with the karst groundwater, are highly efficient in exploring the aquifer system within a specific area and are helpful if combined with other research methods of hydraulic connectivity [24–29]. The valuable perspectives and methods for the exploration of hydraulic connectivity have been obtained by adopting cumbersome mathematical derivation and detailed hydrogeological parameters following the methods described by references [30–38].

The aforementioned methods, which investigate the complex and uncertain hydraulic connectivity, have achieved promising results and have vital practical significance. However, the general quantitative methods of hydraulic connectivity measurements, such as conventional experiments, often have some limitations. These mainly include the long work cycle, the high cost and requirements of adequate data, detailed understanding for hydrogeological parameters, and negative impact on the environment. Meanwhile, most conventional research methods need large-scale and continuous execution. If the conventional experiments are carried out blindly, this will not only enlarge the negative effect of the above shortcomings, but also cause a huge waste of resources. Therefore, the choice of experiment sites is crucial. We should consider whether we can use some methods to select the sites of conventional experiments, which can preliminarily locate the preferential sites of recharge and exploitation. Ultimately, conventional experiments that rely on these preferential sites are implemented. This approach can selectively narrow the scope of experiment sites to optimize the

layouts of recharge and exploitation, thereby decreasing the experimental expenditure and adverse impact on the ecological environment. However, current studies rarely consider a pre-selected issue for experiment sites prior to implementing conventional experiments. Fortunately, even if the relationships between factors are uncertain and the sample size is small, the grey relation analysis method can be utilized. Thus, considered applying this method to reveal the hydraulic connectivity of a complicated karst aquifer system. In light of this, we attempt to present a pre-study method (an improved grey amplitude relation model) to select preliminarily the preferential sites of conventional experiments, which can acquire a series of data to describe hydraulic connectivity quantitatively.

Grey systems theory is one of the widely adopted methods at present, which successfully investigates uncertain problems with limited available information. This method has obvious advantages for handling small sample size and inadequate information [39], and it is not limited by strict requirements for distribution and length of a data sequence and can effectively simplify the calculation process of complex problems [40]. The grey relation degree models are an important part of grey systems theory, and the degree of inter-sequence relations is assessed by measuring the similarity or proximity of the sequences [41]. This model was initially developed in system engineering [42], and since then, different types of grey relation degree models have been widely applied by researchers. The grey absolute relation degree model was first adopted in environmental science to evaluate the relationships of environment and economics [43], and the correlation between pollutants in lake water was investigated utilizing Deng's relation degree [44]. As research progresses, the types of grey relation degree models are further expanded. Dang [45] presented a grey slope incidence model, which was sourced from the slope of a straight line. This model was successfully applied to study the relationship of water tables between different regions [46]. The grey close incidence model was developed in reference [47] to study the influence of human activity on ecological thresholds. The relationship between China's marine–land economy and different sectors were analyzed by using the improved grey periodic relation method [48].

To date, the grey relation degree models were constructed mainly relying on the angle, distance, slope, and change rate of the data sequence; however, they cannot reflect positive and negative correlations. Although the sequence data in real life are usually affected by the dual disturbance of vertical and horizontal coordinates (amplitude and period), the existing research remains less concerned about these two aspects [49]. The grey amplitude relation model was developed by references [50–52] to avoid the aforementioned problems. This model is only affected by the amplitude factors; it can reflect positive and negative correlations and is appropriate for sequence values that have obvious fluctuation trends.

In this paper, the grey amplitude relation model is improved to investigate the groundwater table sequence with an obvious fluctuation trend. To precisely reflect the features of the research object, the data are preprocessed in this study before modeling and the specific calculation period is divided based on the influence factors of groundwater table fluctuation. Accordingly, we present a new quantized index, water table fluctuation relation degree (WTFRD), to preliminarily discuss the hydraulic connectivity of a complex aquifer system. In conclusion, the quantized index WTFRD offers a new insight for the preliminary exploration of hydraulic connectivity. Meanwhile, the improved grey amplitude relation method serves as a viable pre-study method for selecting the preferential sites of conventional experiments. Ultimately, specific experiments are conducted in the preferential sites (with the highest and lowest WTFRD) to verify the hydraulic connectivity. Then, the layouts of recharge and exploration are optimized based on the hydraulic connectivity.

2. Study Area and Data

2.1. Study Area and Hydrogeological Conditions

Jinan, the capital city of Shandong Province, is located in the middle of the province and has an area of 8177.21 km^2. The southern edge of Jinan is close to Mount Tai, and the northern boundary is the Yellow River. Jinan is located in the intersection between the north-west alluvial plains and the south-central low mountains and hills in Shandong Province. Thus, Jinan's terrain distribution has characteristics of high in the south and low in the north. There are many springs in Jinan, thereby leading to its nickname of "Spring City" [53,54]. The main recharge source of karst groundwater in Jinan is rainfall. The average annual rainfall is 647.9 mm, and rainfall is concentrated in June to September each year, which accounts for 70% of the total annual rainfall [55]. Jinan has many springs because of its unique topographic features and geological structure. The karst aquifer system of Jinan is a gentle monoclinic structure with an elevation difference of over 500 m from south to north. This topography is conducive to the surface water and groundwater in southern sections flowing into the northern urban areas [56]. The abundant karst groundwater in Mount Tai flows into the Jinan urban area from south to north, and a large amount of karst groundwater is blocked by impermeable Mesozoic igneous rocks in Northern Jinan and is collected in the contact zone. Under the influence of strong water pressure, karst groundwater flows out forming typical ascending springs through many underground pores, caves, and fractures. Then, many springs outflow perennially in the Jinan urban area and ultimately form Jinan spring groups (Figures 1 and 2). Among many springs in Jinan, Baotu Spring and Black Tiger Spring are the most well-known. However, in recent years, the free outflow rate of both springs has been significantly reduced, and karst groundwater quality deterioration has occurred in the Jinan spring groups due to the over-exploitation of karst groundwater and rapid urbanization [57,58]. Meanwhile, the karst groundwater table in Jinan spring groups has progressively lowered, and some springs have even dried up. In Baotu Spring, the drying-up phenomenon appeared in 1972–2002 (Figure 3). After 2002, a series of spring preservation measures were implemented, which narrowly maintained the continuous outflow of spring water, whereas the outflow rate of springs remained relatively small. Therefore, a potential drying-up crisis occurred during the dry months (from May to June) each year.

Taking effective measures to achieve perennial outflow of the springs and meet the requirements for urban water supply are urgent tasks in Jinan, in which selecting preferential sites to optimize the layout of recharge and exploitation is a critical link. The villages of Dujiamiao, Nanbali, Zhuzhuang, and Kuangli are located in the lower reaches of Yufu River in Western Jinan, which close to the Yufu River and are conducive to the implementation of recharge projects. Therefore, these four villages are selected as our study sequence (for ease of description, the aforementioned four villages are collectively called Western Jinan herein). Moreover, Baotu Spring and Black Tiger Spring in Jinan spring groups are selected as reference sequences. On the basis of the karst groundwater table data of Western Jinan and Jinan spring groups, the preferential sites of conventional experiments are selected by using the quantized index WTFRD. Ultimately, the layout of recharge and exploration will be optimized. The locations of Western Jinan and Jinan spring groups are shown in Figure 1.

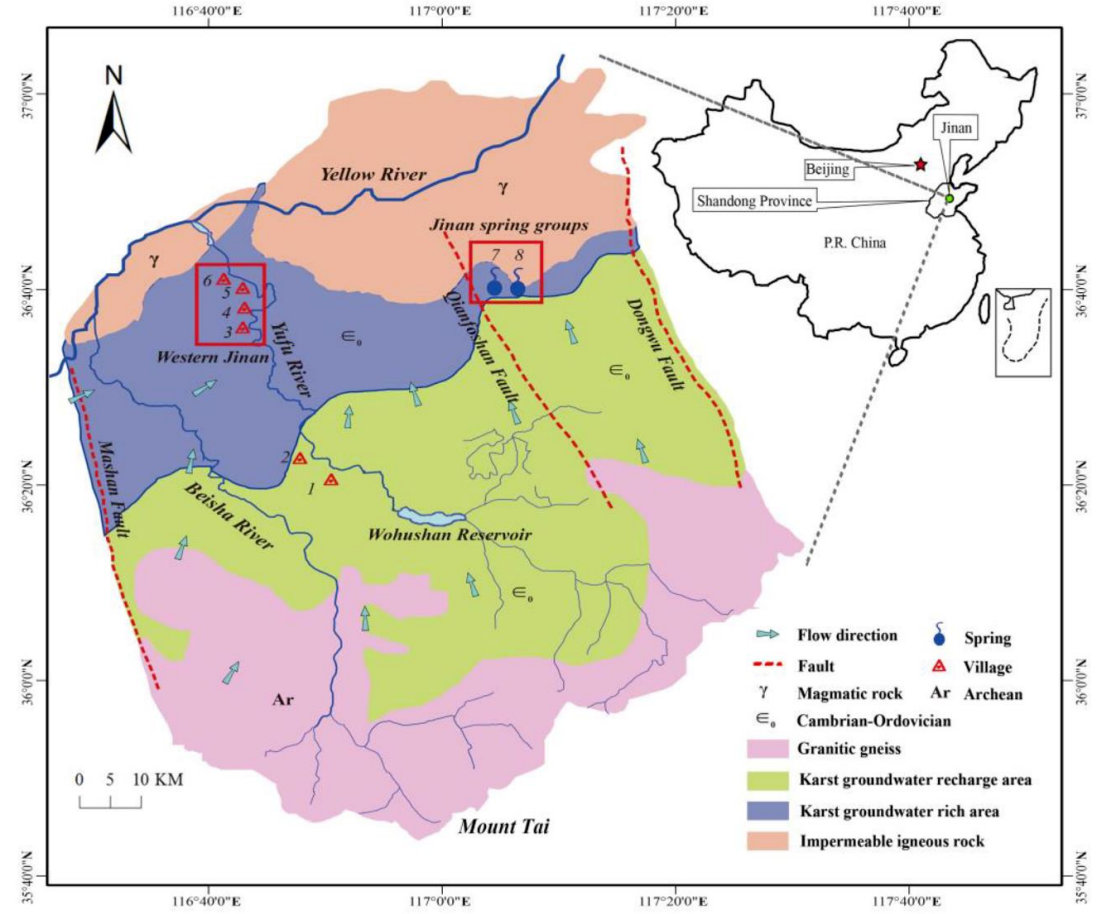

Figure 1. Location map of Jinan spring catchment shows 1—Cuima Village, 2—Yinjialin Village, 3—Dujiamiao Village, 4—Zhuzhuang Village, 5—Nanbali Village, 6—Kuangli Village, 7—Baotu Spring, 8—Black Tiger Spring.

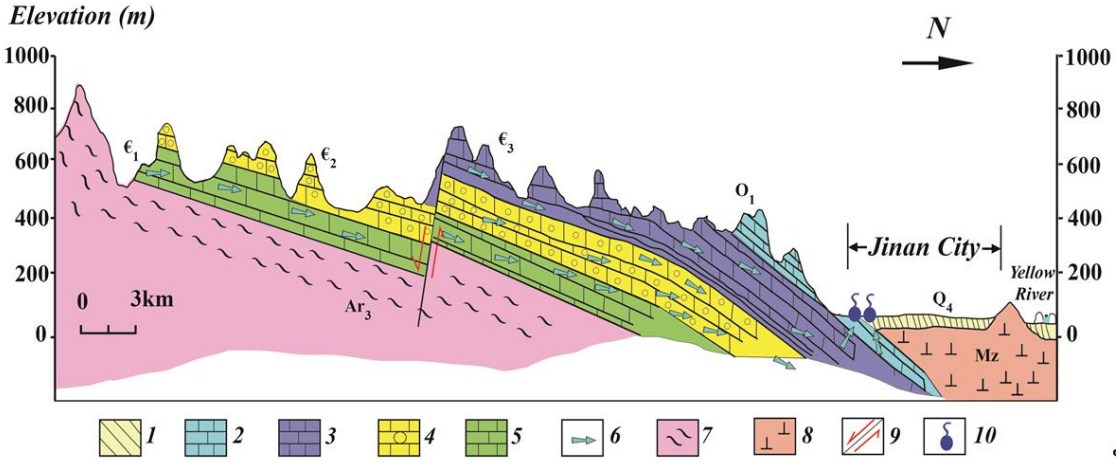

Figure 2. Geological longitudinal section of Jinan spring catchment shows 1—Soil (Q_4), 2—Dolomitic limestone (O_1), 3—Limestone and shale ($€_3$), 4—Oolitic limestone ($€_2$), 5—Limestone and shale ($€_1$), 6—Flow direction, 7—Granitic gneiss (Ar_3), 8—Diorite (M_Z), 9—Fault, 10—Jinan spring groups; (Q_4 is Quaternary sediment, O_1 is Lower Ordovician, $€_1$ is Lower Cambrian, $€_2$ is Middle Cambrian, $€_3$ is Upper Cambrian, Ar_3 is Archean, M_Z is Mesozoic).

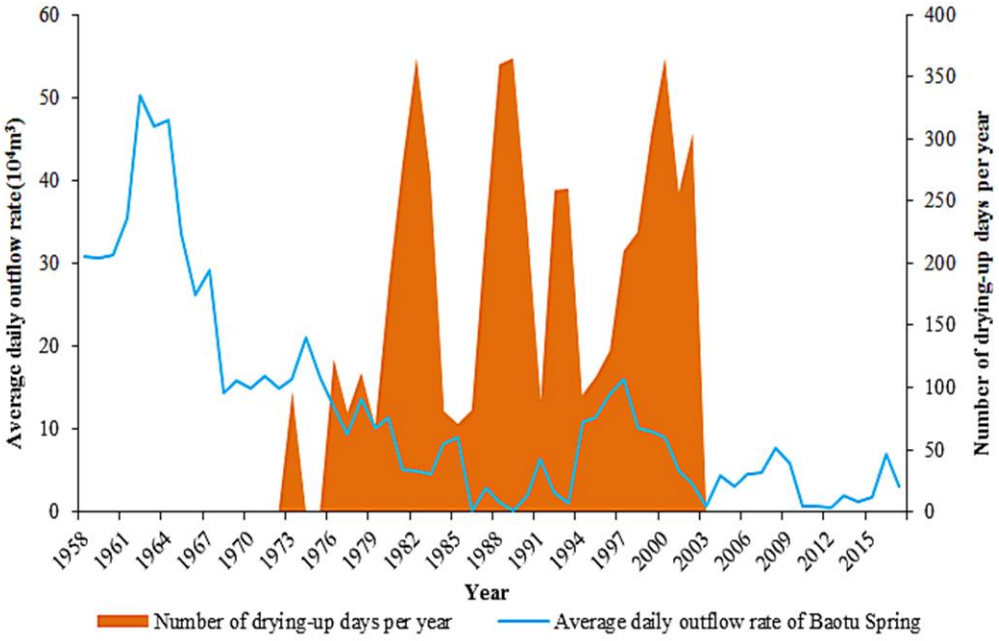

Figure 3. Outflow rate and number of drying-up days in Baotu Spring.

2.2. Analysis of Fluctuant Law and Influence Factor in Karst Groundwater Table

The fluctuant law of karst groundwater table in Jinan spring catchment shows a beginning of decline in March each year, and the most obvious and fast decline is from May to June. The main reason is that temperature increases rapidly with the arrival of springtime after March, and the weather becomes increasingly dry. Meanwhile, little rainfall and strong evaporation make the soil lose considerable moisture. From May to June, a large-scale karst groundwater is artificially extracted for agricultural irrigation with the beginning of spring plowing in Western Jinan, which results in a significant decline of karst groundwater table. After that, the karst groundwater table is raised gradually along with the ending of spring plowing after July and does not reach a maximum until September (Figure 4). In addition, Jinan belongs to the warm temperate zone monsoon climate, in which the optimal sowing date of winter wheat is from October to November. Therefore, winter wheat irrigation makes the karst groundwater table fall back again after October in Western Jinan. To recover the karst groundwater resources in Western Jinan effectively, the government has conducted a regional-scale aquifer recharge project in Yufu River to convert surface water into karst groundwater. This measure has a positive effect on the replenishment of karst groundwater in Western Jinan, especially during agricultural irrigation (April to July and October to November). Thus, the variable law of karst groundwater table is fairly complex in Jinan spring catchment; its main influence factors include rainfall, artificial recharge, and extraction. The month-to-month movement of karst groundwater table, rainfall, and recharge quantity from 2014 to 2017 is shown in Figure 4. Basic information and statistical characteristics of karst groundwater table data are shown in Table 1. These data are derived from the Jinan Hydrology Bureau, Shandong Province. The fluctuation law of karst groundwater table between Jinan spring groups and Western Jinan is consistent. In addition, the karst groundwater table of Western Jinan is slightly higher than that of Jinan spring groups. Therefore, we suspect that hydraulic connectivity may occur between Western Jinan and Jinan spring groups. Karst groundwater recharge in Western Jinan may contribute to the elevation of the karst groundwater table in Jinan spring groups.

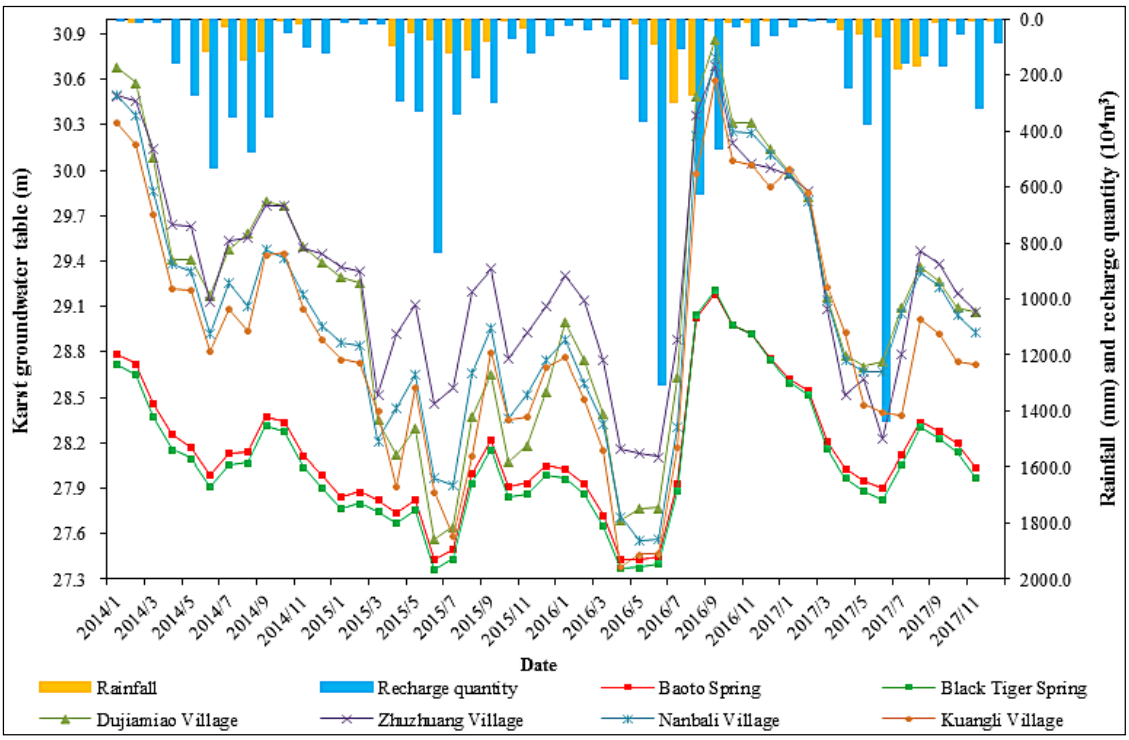

Figure 4. Condition of karst groundwater table, rainfall and recharge quantity from 2014 to 2017.

Table 1. Basic information and statistical characteristics of karst groundwater table data.

Statistics		Baoto Spring	Black Tiger Spring	Dujiamiao Village	Zhuzhuang Village	Nanbali Village	Kuangli Village
Missing value		0.000	0.000	0.000	0.000	0.000	0.000
Mean		28.141	28.084	29.114	29.289	29.043	28.885
Median		28.050	27.989	29.157	29.305	28.955	28.800
Mode		27.989 [a]	27.367 [a]	27.563 [a]	28.108 [a]	27.553 [a]	27.385 [a]
Minimum		27.427	27.367	27.563	28.108	27.553	27.385
Maximum		29.185	29.211	30.859	30.692	30.745	30.590
Range		1.758	1.844	3.296	2.584	3.192	3.205
Standard error of Mean		0.063	0.065	0.126	0.096	0.113	0.116
Variance		0.184	0.199	0.744	0.430	0.600	0.627
Standard deviation		0.429	0.446	0.863	0.656	0.775	0.792
Skewness		0.523	0.657	0.079	0.134	0.231	0.165
Standard error of Skewness		0.347	0.347	0.347	0.347	0.347	0.347
Kurtosis		0.043	0.189	−0.680	−0.522	−0.289	−0.449
Standard error of Kurtosis		0.681	0.681	0.681	0.681	0.681	0.681
Percentiles	10	27.488	27.429	27.769	28.411	27.958	27.819
	50	28.050	27.989	29.157	29.305	28.955	28.800
	90	28.809	28.778	30.349	30.220	30.251	30.038

[a] indicates the minimum value of the Mode when multiple Modes present.

As shown in Table 2, the rainfall in 2014 and 2015 was 444 mm and 572.8 mm, which belongs to the extremely dry and dry years, respectively. Sustained low rainfall resulted in water shortages in Jinan. To realize perennial outflow of the springs and meet the requirements for urban water supply, a three-stage contingency plan was launched in Jinan. Meanwhile, the karst groundwater extraction was strictly controlled, and the artificial recharge measures were gradually performed (artificial recharge quantity data are provided by Jinan City Qingyuan Water Group Co. Ltd., Jinan, China). Little rainfall resulted in a relatively dry climate over the past four years, except for 2016. Thus, the infiltration recharge by rainfall in Jinan spring catchment was rather less, which made the karst groundwater table of Baotu Spring and Black Tiger Spring lower than the yellow warning line of the water table

(28.15 m) in the Jinan Springs Protection Ordinance. The total rainfall and artificial recharge quantity in 2016 and 2017 did not appear as a significant increase; therefore, the groundwater funnel caused by over-exploitation could not be completely repaired during the short period. This means the current situation of spring water protection and water supply in Jinan is not optimistic.

Table 2. Total rainfall and artificial recharge quantity from 2014 to 2017.

Year	Total Rainfall in Jinan (mm)	Abundance or Shortage of Rainfall	Artificial Recharge Quantity in Western Jinan (10^4 m^3)
2014	444	Extremely dry year	2439.3
2015	572.8	Dry year	2608.4
2016	710.8	Normal precipitation year	3372.85
2017	520.5	Dry year	3024.06

3. Methods

3.1. Basic Thinking in the Improved Grey Amplitude Relation Model

In water resource engineering, the investigations of aquifer systems have often become extremely difficult due to incomplete parameters, structures, boundaries and uncertain hydraulic characteristics. In addition, the fluctuation causes of karst groundwater table are also complex. Therefore, the aquifer systems can be regarded as a grey system. Recharge or extraction of karst groundwater in one area may contribute to the rise or fall of karst groundwater table in another area. Although the fluctuation periods (the interval of time sequence i.e., abscissa) of karst groundwater table between the two areas are different, the fluctuation amplitudes are similar. If the correlation of fluctuation amplitudes is investigated using conventional grey relation degree models, then the period and amplitude of waves will be considered as common influencing factors on the karst groundwater table. This situation will inevitably reduce the accuracy of the analysis and may even lead to incorrect results. Therefore, eliminating the noise of the fluctuation period when studying the correlation of fluctuation amplitudes is necessary. Thus, this study combines the grey relation degree models with the fluctuation characteristics of karst groundwater table and then develops an improved grey amplitude relation model. This model only considers the fluctuation amplitudes between the two sequences and eliminates the interference of other factors, such as the fluctuation period. Overall, the improved grey amplitude relation model generally outperforms conventional grey relation degree models, which is well suited for dealing with the karst groundwater table sequence with an obvious fluctuation trend. Finally, we attempt to preliminarily explore the hydraulic connectivity of a complex karst aquifer system using the proposed model.

3.2. Development of the Improved Grey Amplitude Relation Model

3.2.1. Data Preprocessing

First, the average karst groundwater table is calculated with a 15-day cycle (because the groundwater table data are artificially measured and limited by the sampling period), and time series values are obtained. We assume that the time series values in Jinan spring groups are $Y_1 = (y_1, y_2, \ldots, y_i, \ldots, y_n)$ and those of Western Jinan are $Y_j = (y_1^*, y_2^*, \ldots, y_i^*, \ldots, y_n^*)$.

Each time series value (y) in Y corresponds to a time value (x); thus, the time sequence $X = (x_1, x_2, \ldots, x_i, \ldots, x_n)$ can be obtained.

3.2.2. Creation of the Polyline

Setting the time sequence $X = (x_1, x_2, \ldots, x_i, \ldots, x_n)$, where $1 \leq i \leq n$, the time sequence X corresponds to time series values $Y_1 = (y_1, y_2, \ldots, y_i, \ldots, y_n)$; the two-dimensional Cartesian

coordinate system is developed using X as the abscissa and Y_1 as the ordinate, and then connecting each point (x_i, y_i) to structure a polyline L_1 in a two-dimensional Cartesian coordinate system (Figure 5).

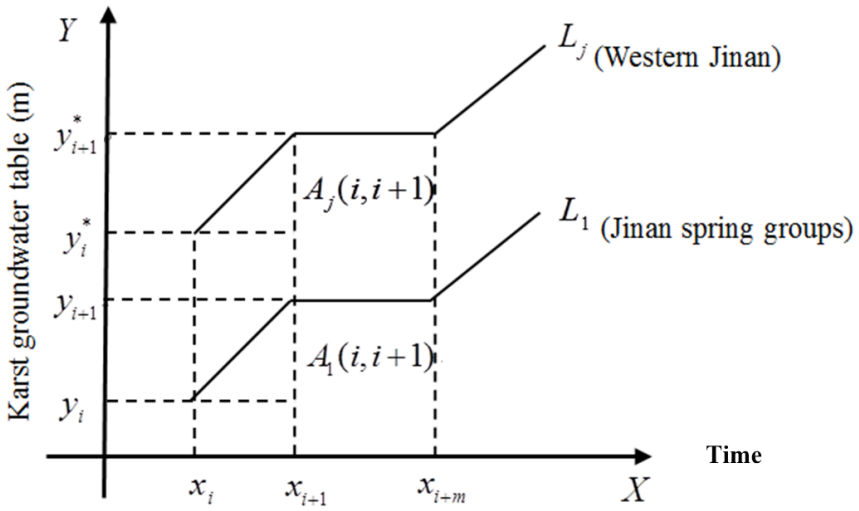

Figure 5. Relationship between the polyline coordinate and the fluctuation amplitude values.

Likewise, the time sequence X corresponds to time series values $Y_j = (y_1^*, y_2^*, \ldots, y_i^*, \ldots, y_n^*)$, connecting each point (x_i, y_i^*) to structure a polyline L_j in a two-dimensional Cartesian coordinate system (Figure 5).

3.2.3. Calculation of the Fluctuation Amplitude Values

The fluctuation amplitude values are calculated by Equation (1).

$$A_1(i, i+1) = y_{i+1} - y_i = \Delta Y_1(i), \tag{1}$$

where $A_1(i, i+1)$ and $\Delta Y_1(i)$ are the fluctuation amplitude values of Jinan spring groups, and y_i and y_{i+1} are the ordinate (karst groundwater table) of the polyline $L_1(i, i+1)$.

Similarly, the fluctuation amplitude values of the polyline $L_j(i, i+1)$ are

$$A_j(i, i+1) = y_{i+1}^* - y_i^* = \Delta Y_j(i), \tag{2}$$

where $A_j(i, i+1)$ and $\Delta Y_j(i)$ are the fluctuation amplitude values of Western Jinan, and y_i^* and y_{i+1}^* are the ordinate (karst groundwater table) of the polyline $L_j(i, i+1)$.

3.2.4. Calculation of the Water Table Fluctuation Relation Coefficient

The water table fluctuation relation coefficient of the ith wave between polylines L_1 and L_j is

$$R_{1,j}(i) = \mathrm{sgn}(A_1(i, i+1), A_j(i, i+1)) * \frac{1+|A_1(i,i+1)|+\left|A_j(i,i+1)\right|}{1+|A_1(i,i+1)|+\left|A_j(i,i+1)\right|+\left||A_1(i,i+1)|-\left|A_j(i,i+1)\right|\right|}, \tag{3}$$

$$\mathrm{sgn}(A_1(i, i+1), A_j(i, i+1)) = \begin{cases} +1, & A_1(i, i+1) * A_j(i, i+1)) \geq 0 \\ -1, & A_1(i, i+1) * A_j(i, i+1)) < 0 \end{cases} \tag{4}$$

where $A_1(i, i+1)$ is the fluctuation amplitude value of the polyline L_1, $A_j(i, i+1)$ is the fluctuation amplitude value of the polyline L_j, and $R_{1,j}(i)$ is the water table fluctuation relation coefficient between polylines L_1 and L_j.

3.2.5. Calculation of WTFRD

The WTFRD between Jinan spring groups (polyline L_1) and Western Jinan (polyline L_j) is

$$\gamma_{1,j} = \frac{1}{k}\sum_{i=1}^{k} w_i R_{1,j}(i), \tag{5}$$

where $R_{1,j}(i)$ is the water table fluctuation relation coefficient between polylines L_1 and L_j, k is the sample size of $R_{1,j}(i)$, $\gamma_{1,j}$ is the WTFRD between polylines L_1 and L_j, and w_i is the weight of each indicator (this study adopts equal weight calculation; as is customary, the value of w_i can be calculated using the subjective, objective, or combinatorial weighting methods based on actual requirements).

3.2.6. Property of WTFRD

(i) Water table fluctuation relation coefficient ($R_{1,j}(i)$) and WTFRD ($\gamma_{1,j}$) are only subjected to magnitude and direction of the fluctuations amplitude, which are unaffected by other factors, such as sequence abscissa X. They are highly suited to investigate the relationship between two sequences with obvious fluctuation trends in complex systems.

(ii) The existence of a complete positive correlation between two waves ($R_{1,j}(i) = 1$) when the magnitude and direction of the amplitude between the two waves are equal.

$$\begin{aligned} R_{1,j}(i) &= \mathrm{sgn}(A_1(i,i+1), A_j(i,i+1)) * \frac{1+|A_1(i,i+1)|+\left|A_j(i,i+1)\right|}{1+|A_1(i,i+1)|+\left|A_j(i,i+1)\right|+\left||A_1(i,i+1)|-\left|A_j(i,i+1)\right|\right|} \\ &= \frac{1+|A_1(i,i+1)|+\left|A_j(i,i+1)\right|}{1+|A_1(i,i+1)|+\left|A_j(i,i+1)\right|+\left||A_1(i,i+1)|-\left|A_j(i,i+1)\right|\right|} \\ &= \frac{1+|A_1(i,i+1)|+\left|A_j(i,i+1)\right|}{1+|A_1(i,i+1)|+\left|A_j(i,i+1)\right|} \\ &= 1 \end{aligned}$$

(iii) A complete negative correlation occurs between two waves ($R_{1,j}(i) = -1$) when the equal magnitude and the opposite direction occur within amplitudes.

$$\begin{aligned} R_{1,j}(i) &= \mathrm{sgn}(A_1(i,i+1), A_j(i,i+1)) * \frac{1+|A_1(i,i+1)|+\left|A_j(i,i+1)\right|}{1+|A_1(i,i+1)|+\left|A_j(i,i+1)\right|+\left||A_1(i,i+1)|-\left|A_j(i,i+1)\right|\right|} \\ &= (-1) * \frac{1+|A_1(i,i+1)|+\left|A_j(i,i+1)\right|}{1+|A_1(i,i+1)|+\left|A_j(i,i+1)\right|+\left||A_1(i,i+1)|-\left|A_j(i,i+1)\right|\right|} \\ &= (-1) * \frac{1+|A_1(i,i+1)|+\left|A_j(i,i+1)\right|}{1+|A_1(i,i+1)|+\left|A_j(i,i+1)\right|} \\ &= -1 \end{aligned}$$

(iv) If and only if $A_1(i,i+1) = A_j(i,i+1)$, then $R_{1,j}(i) = \pm 1$; and $A_1(i,i+1) = A_j(i,i+1) = 0$, $\gamma_{1,j} = 1$. Furthermore, the numerator of $R_{1,j}(i)$ is not greater than the denominator, that is, $(1 + |A_1(i,i+1)| + |A_j(i,i+1)| \leq 1 + |A_1(i,i+1)| + |A_j(i,i+1)| + ||A_1(i,i+1)| - |A_j(i,i+1)||)$; thus, $-1 \leq R_{1,j}(i) \leq 1$ and $-1 \leq \gamma_{1,j} \leq 1$.

(v) A high absolute value of WTFRD indicates a strong correlation. If $|\gamma_{0,1}| > \left|\gamma_{0,j}\right|$, then the correlation between L_0 and L_1 is stronger than that of L_0 and L_j.

3.2.7. Grading WTFRD

The interval range of WTFRD is $[-1, 1]$. This study takes interval $[0, 1]$ as an example (the situation of interval $[-1, 0]$ is similar to that of interval $[0, 1]$), which is divided into four subintervals; each subinterval is set with a group of relation degree grades (Table 3). Finally, the correlation between

study sequence and reference sequence is evaluated according to the WTFRD grade. If the calculation results of the WTFRD appear in the negative values, a negative correlation occurs between study sequence and reference sequence. The results are not listed in this paper, and their classification is similar to that of Table 3.

Table 3. Grading of water table fluctuation relation degree (WTFRD) [59,60].

WTFRD	Grade Division	Evaluative Meaning
0–0.3	Low relation degree	Study sequence deviates greatly from the reference sequence
0.3–0.6	Medium relation degree	Certain deviation exists between study sequence and reference sequence
0.6–0.8	Relatively strong relation degree	Study sequence is close to the reference sequence
0.8–1.0	High relation degree	Study sequence is extremely close to the reference sequence

4. Results

4.1. Analysis of Whole-Year WTFRD

The variable law of karst groundwater table for Western Jinan and Jinan spring groups in 2014–2017 was carefully analyzed. The WTFRD between the two study sites over the past four years was calculated using Equations (1)–(5). The whole-year WTFRD between Western Jinan and Jinan spring groups is shown in Table 4.

Table 4. Whole-year WTFRD from 2014 to 2017.

Site	Dujiamiao Village	Zhuzhuang Village	Nanbali Village	Kuangli Village	Whole-Year WTFRD
Baotu Spring	0.710	0.694	0.673	0.711	0.697
Black Tiger Spring	0.669	0.650	0.675	0.713	0.677

The calculation results in Table 4 indicate that the whole-year WTFRD of Baotu Spring–Western Jinan and of Black Tiger Spring–Western Jinan are 0.697 and 0.677, respectively, which are both greater than 0.6. In comparison with Table 3, the values belong to the relatively strong relation degree grade, which indicates there is the correlation of karst aquifer between Western Jinan and Jinan spring groups from the angle of statistics. However, the whole-year WTFRD is not high enough. It is insufficiently convincing to explore hydraulic connectivity using only these results.

To further explore the interaction mechanism and main driving force of the karst aquifer between Western Jinan and Jinan spring groups, the time series values by month were divided into three different periods (April to July, August to November, and December to March of next year) based on the conditions of rainfall and artificial recharge and exploitation in Jinan. Then, WTFRD was calculated in specific periods.

4.2. Analysis of WTFRD in Different Periods

4.2.1. Rainfall and Karst Groundwater Recharge during Different Periods

Empirical studies show that the main influence factors on karst groundwater table in Jinan are rainfall, artificial recharge, and exploitation [61–63]. The distribution of rainfall is nearly homogeneous in Jinan; thus, the rainfall of Jinan spring groups and Western Jinan is regarded as the same condition in this paper. By contrast, the recharge and exploitation of karst groundwater are only conducted in Western Jinan. Based on the above three different periods, rainfall and recharge quantity from 2014 to 2017 were investigated (Table 5). A rough analysis shows that the general distribution of rainfall

in all years is as follows: August to November > April to July > December to March of next year. The distribution of recharge quantity in all years is as follows: April to July > August to November > December to March of next year. At present, Jinan's agriculture is mainly concentrated in Western Jinan; karst groundwater is the main irrigation water source. The primary crops are vegetables, wheat, and corn, which are grown in Western Jinan for two seasons every year (especially wheat). Karst groundwater is extracted for agricultural irrigation during the planting season. Therefore, karst groundwater exploitation mainly focuses on two periods annually, that is, April to July and October to November. From April to July, the spring plowing is carried out in Western Jinan, and the main crops are vegetables, wheat, and corn. The planting scale is relatively large, and the water requirement is considerable; thus, the quantity and scale of karst groundwater exploitation are the largest in a year. From October to November, the crops in Western Jinan are mainly winter wheat, and the planting scale is less than that of spring plowing. Therefore, the exploitation quantity of karst groundwater during the winter wheat irrigation is considerably smaller than that of spring plowing. From December to March of next year, the winter wheat in Western Jinan hardly requires irrigation, which means the karst groundwater is extracted slightly. The investigation and analysis indicate that the current situation of karst groundwater exploitation in Western Jinan is as follows: April to July > August to November > December to March of next year. Overall, rainfall, recharge, and exploitation are the lowest from December to March of next year.

Table 5. Rainfall and artificial recharge quantity during different periods.

Year	Rainfall in Jinan (mm)			Artificial Recharge Quantity in Western Jinan (10^4 m^3)			Exploitation in Western Jinan
	April toJuly	August to November	December to March	April to July	August to November	December to March	
2014	153.6	290.4	0	1310	977	32.6	Mainly concentrated in April to July and October to November each year (the specific data were not announced)
2015	340.2	232.6	0	1800.2	701	49.2	
2016	358	352.8	0	2001.1	1220.09	209.67	
2017	186.9	330.6	4.5	2118.7	678.46	104.53	

4.2.2. WTFRD Analysis from April to July Each Year

The annual start of spring plowing in Western Jinan after April results in a large quantity of karst groundwater being exploited for agricultural irrigation. Therefore, the calculation result of WTFRD might be affected by large-scale karst groundwater exploitation during this period.

First, the annual WTFRD between the Baotu Spring, Black Tiger Spring and the four villages were calculated. Then the annual average WTFRD between Western Jinan and Jinan spring groups could be obtained. Further, the piecewise WTFRD were calculated using the mean value of the annual average WTFRD from 2014 to 2017. As shown in Tables 4 and 6, the annual average WTFRD from April to July each year is generally smaller than the whole-year WTFRD. Combining Table 5, the spring plowing in Western Jinan causes large-scale karst groundwater to be extracted for agricultural irrigation from April to July each year. In addition, the water consumption of agriculture irrigation is mainly affected by rainfall and the water demand of crops. The artificial irrigation is needed when the water demand of crops is relatively large while little rainfall occurs. This situation will lead to the massive exploitation of karst groundwater. Table 6 shows that the piecewise WTFRD of Western Jinan–Baotu Spring and of Western Jinan–Black Tiger Spring are 0.419 and 0.388, respectively. These values are relatively small, both of which are in medium relation degree grade.

Table 6. WTFRD between Western Jinan and Jinan spring groups from April to July each year.

Site	Year	Dujiamiao Village	Zhuzhuang Village	Nanbali Village	Kuangli Village	Annual Average WTFRD	Piecewise WTFRD
Baotu Spring	2014	0.393	0.364	0.088	0.098	0.236	0.419
	2015	0.641	0.664	0.918	0.661	0.721	
	2016	0.929	0.936	0.121	0.386	0.593	
	2017	0.129	0.161	0.130	0.085	0.126	
Black Tiger Spring	2014	0.112	0.336	0.091	0.096	0.159	0.388
	2015	0.639	0.596	0.917	0.659	0.703	
	2016	0.924	0.845	0.124	0.382	0.569	
	2017	0.130	0.143	0.130	0.087	0.122	

Furthermore, we conducted a detailed investigation by combining the conditions of rainfall, artificial recharge, and extraction to explore the main reason for low piecewise WTFRD from April to July each year. On the one hand, the intra-annual analysis of the annual average WTFRD indicates that the rainfall from April to July each year is generally small, although the exploitation quantity of karst groundwater is the maximum during this period. The annual average WTFRD in this period is significantly lower than that of August to November and of December to March of next year (combined with the annual average WTFRD in Tables 6–8) due to the hysteretic nature of karst groundwater movement between Western Jinan and Jinan spring groups. On the other hand, the inter-annual analysis of annual average WTFRD shows that: (i) The artificial recharge quantity from April to July in 2016 and 2017 are extremely close. By contrast, the rainfall from April to July in 2017 is significantly lower than that of 2016, thereby resulting in the karst groundwater extraction from April to July in 2017 being greater than that of 2016. Therefore, the annual average WTFRD from April to July in 2016 is considerably higher than that of 2017. (ii) The rainfall from April to July in 2014 and 2017 is extremely close, whereas the artificial recharge quantity from April to July in 2014 is significantly less than that of 2017; ultimately, the annual average WTFRD from April to July in 2014 is slightly higher than that of 2017 (Tables 5 and 6).

In view of this, the influence factors of piecewise WTFRD between Western Jinan and Jinan spring groups from April to July each year were investigated based on the current conditions (the rainfall, artificial recharge, and extraction) in Western Jinan. The results indicate that the effect of artificial recharge on piecewise WTFRD is relatively small, whereas the effect of exploitation on it is larger than recharge. Therefore, low piecewise WTFRD from April to July each year is mainly affected by exploitation in Western Jinan.

Table 7. WTFRD between Western Jinan and Jinan spring groups from August to November each year.

Site	Year	Dujiamiao Village	Zhuzhuang Village	Nanbali Village	Kuangli Village	Annual Average WTFRD	Piecewise WTFRD
Baotu Spring	2014	0.677	0.968	0.685	0.948	0.820	0.820
	2015	0.917	0.937	0.918	0.926	0.925	
	2016	0.661	0.654	0.641	0.646	0.650	
	2017	0.960	0.673	0.959	0.956	0.887	
Black Tiger Spring	2014	0.680	0.618	0.689	0.952	0.735	0.772
	2015	0.915	0.853	0.917	0.925	0.902	
	2016	0.668	0.588	0.645	0.650	0.638	
	2017	0.680	0.663	0.960	0.957	0.815	

Table 8. WTFRD between Western Jinan and Jinan spring groups from December to March of next year.

Site	Year	Dujiamiao Village	Zhuzhuang Village	Nanbali Village	Kuangli Village	Annual Average WTFRD	Piecewise WTFRD
Baotu Spring	2014	0.949	0.943	0.938	0.940	0.943	0.846
	2015	0.623	0.919	0.933	0.953	0.857	
	2016	0.624	0.909	0.648	0.932	0.778	
	2017	0.662	0.938	0.946	0.678	0.806	
Black Tiger Spring	2014	0.957	0.934	0.951	0.959	0.950	0.861
	2015	0.903	0.899	0.930	0.950	0.920	
	2016	0.626	0.898	0.646	0.931	0.775	
	2017	0.666	0.900	0.949	0.681	0.799	

4.2.3. WTFRD Analysis from August to November Each Year

There is an abundant rainfall from August to September each year, and the small-scale karst groundwater is extracted to plant winter wheat from October to November. Hence, the change of karst groundwater table in Western Jinan is likely to be affected by exploitation, rainfall, and artificial recharge. Table 7 presents the WTFRD.

The recharge and discharge of karst groundwater in Western Jinan is complicated from August to November each year. Jinan enters the rainy season with rich rainwater from August to September; thus, karst groundwater in Western Jinan is effectively fed. At the beginning of October to November, the winter wheat enters into an optimal sowing period, which results in karst groundwater being extracted for winter wheat irrigation in Western Jinan. The quantity of pumping water is considerably smaller than that of spring plowing (from April to July) because of the small planting scale and short pumping time. Therefore, the effect of exploitation on WTFRD during this period is less than that during spring plowing.

The piecewise WTFRD between Western Jinan and Jinan spring groups are 0.820 and 0.772 from August to November (Table 7), which belong to the high relation degree and the relatively strong relation degree grades, respectively. Moreover, the annual average WTFRD in 2016 is obviously lower than that of other years. The main reason is the recharge quantity from August to November in 2016 (the recharge quantity of 1220.09 $\times$ 10^4 m^3 is the maximal over the past four years) that reduces the annual average WTFRD during this period. Accordingly, artificial recharge is the main influence factor for piecewise WTFRD from August to November, followed by rainfall and winter wheat irrigation.

4.2.4. WTFRD Analysis from December to March of Next Year

Winter in Jinan occurs from December to March of next year, in which the karst groundwater table is rarely influenced by rainfall and exploitation. To realize the perennial outflow of Jinan spring groups and guarantee water demand of large-scale agricultural irrigation (from April to July), as well as to ease the declining trend of karst groundwater table, the karst groundwater recharge project was launched in Jinan City. Table 8 shows that the piecewise WTFRD of Western Jinan–Baotu Spring and Western Jinan–Black Tiger Spring are 0.846 and 0.861, respectively. In addition, the annual average WTFRD is relatively close, and only the annual average WTFRD of 2016 is slightly lower than that of other years. Meanwhile, the artificial recharge quantity (209.67 $\times$ 10^4 m^3) from December 2016 to March of next year is larger than that of other years (Table 5). The annual average WTFRD from December to March of next year is reduced by the artificial recharge due to the hysteretic nature of karst groundwater movement. Hence, the piecewise WTFRD from December to March of next year is mainly affected by artificial recharge, while the influence of rainfall and exploitation on piecewise WTFRD is smaller.

4.3. Analysis of Total WTFRD

The total WTFRD was calculated using the mean value of piecewise WTFRD based on the piecewise WTFRD in Tables 6–8 (under the entire year condition, the total WTFRD is the mean value of the whole-year WTFRD in Table 4). As shown in Table 9, the total WTFRD between Western Jinan and Jinan spring groups are in the following order: April to July (0.404) < Entire year (0.687) < August to November (0.796) < December to March of next year (0.854). Analysis and comparisons show that the total WTFRD from April to July each year is greatly affected by spring plowing with a value of only 0.404. Furthermore, the total WTFRD in the other months (August to November and December to March of next year) is mainly affected by small-scale recharge. The total WTFRD between Western Jinan and Jinan spring groups are 0.796 and 0.854 during this period, which belong to relatively strong relation degree and high correlation grades, respectively.

Table 9. Analysis of total WTFRD and its influence factors.

Period	Influence Factors of WTFRD	Major Factor	Total WTFRD	Grade Division
April to July	Rainfall, exploitation, artificial recharge	Exploitation	0.404	Medium relation degree
August to November	Rainfall, exploitation, artificial recharge	Artificial recharge	0.796	Relatively strong relation degree
December to March of next year	Rainfall, artificial recharge	Artificial recharge	0.854	High relation degree
Entire year	Rainfall, exploitation, artificial recharge	Exploitation	0.687	Relatively strong relation degree

In addition, the total WTFRD of entire year is 0.687, which is greater than 0.6; this value is in the relatively strong relation degree grade. For the entire year, the influence factors of total WTFRD include seasonal exploitation, rainfall and artificial recharge, in which seasonal exploitation is the major factor, followed by rainfall and artificial recharge. The total WTFRD was calculated under the rarely disturbed conditions by excluding the interference of seasonal exploitation (spring plowing and winter wheat irrigation) in this study. The karst groundwater table from December to March of next year is hardly affected by artificial factors. Thus, the total WTFRD in this period provides a more scientific and reliable basis for exploring the hydraulic connectivity of aquifer system between Western Jinan and Jinan spring groups. The total WTFRD in this period is 0.854, which is greater than 0.8; this value belongs to the high relation degree grade. This result indicates that high hydraulic connectivity occurs between Western Jinan and Jinan spring groups under the condition of the minimum external disturbance from the view of statistics. Meanwhile, the fluctuation law of karst groundwater table between Western Jinan and Jinan spring groups is similar (Figure 4). Accordingly, Western Jinan can be regarded as preferential sites for performing conventional experiments to investigate the hydraulic connectivity between Western Jinan and Jinan spring groups and reveal whether these sites can be used as the optimal sites for karst groundwater recharge.

4.4. Case Verification

Two sites (Cuima and Yinjialin Villages) with known hydraulic connectivity are selected to verify the validity and precision of this model using the karst groundwater tables of these sites from 2014 to 2016. Cuima Village is located in the upper reaches of Yinjialin Village, and their change rule of karst groundwater table is the same (Figures 1 and 6). The hydraulic connectivity between Cuima and Yinjialin Villages is verified by the environmental isotope tracing technique [64,65]. The WTFGD is 0.822 from 2014 to 2016, which is in the high relation degree grade. This value is consistent with the actual experimental results, which indicates that the improved grey amplitude relation method and the WTFRD index are reasonable.

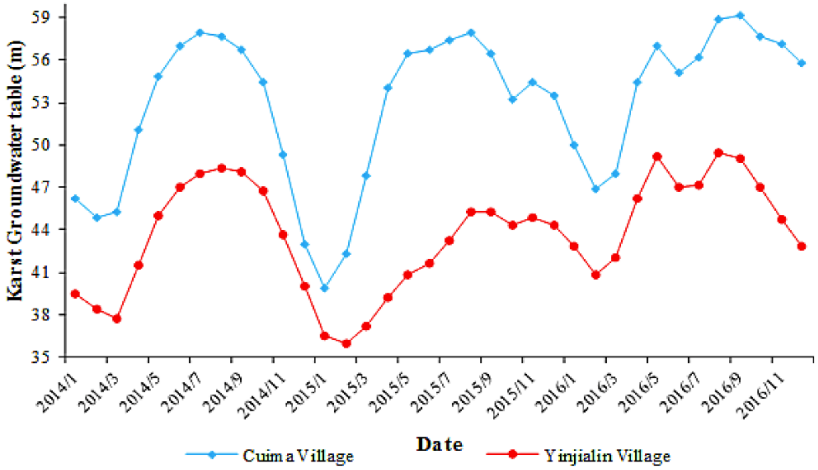

Figure 6. Conditions of karst groundwater table in Cuima and Yinjialin Villages from 2014 to 2016.

However, we only use karst groundwater table data between two areas to study hydraulic connectivity without considering regional hydrogeological conditions. Evaluating hydraulic connectivity relying on the conclusions obtained by this method is insufficiently convincing. Given the original aims of this study, we consider the improved grey amplitude relation method as a pre-study method of conventional experiments and attempt to draw on advantages of different methods to form a high-efficiency and low-cost combined method. If this process is conducted, then we can improve the selection accuracy of the conventional experiment sites and can narrow the scope of the experiment sites, thereby further effectively reducing the experimental cost and the negative impact on the ecological environment.

5. Discussion

To protect springs and supply water, Jinan urgently needs to determine as soon as possible the hydraulic connectivity between Jinan spring groups and other regions. The karst groundwater recharge project can be conducted in the regions with the high hydraulic connectivity to restore the karst groundwater resources in Jinan spring groups effectively. Meanwhile, the karst groundwater will be exploited in the regions with the low hydraulic connectivity (the minimum influence on Jinan spring groups' aquifer) for urban water supply. To study the hydraulic connectivity, many conventional experiments are implemented blindly and subjectively; these experiments have a long work cycle, a high cost, and some negative effects on the environment and human health. In this context, we attempt to apply the improved grey amplitude relation method that is a pre-study of conventional experiments to explore initially the hydraulic connectivity of the aquifer system, and the preferential sites are further selected to implement conventional experiments. This method has the features of simple calculation and convenient operation. It also has the following advantages: (i) It only considers the fluctuation amplitudes between two sequences and eliminates the interference of other factors, such as the fluctuation period, which is suited for dealing with the water table sequence with an obvious fluctuation trend; (ii) the method provides a quantitative study for hydraulic connectivity of a complex aquifer system; (iii) it does not need many hydrogeological parameters in the calculation process, while it only needs the karst groundwater table data of existing observation wells; (iv) this method does not consume massive labor, physical resources, and finances; (v) it does not use any hydrochemistry ions and environmental isotope tracers, so it will not produce any negative effect on the ecological environment and aquifer systems as well as on the daily life of neighboring residents. Ultimately, the scope of conventional experimental sites is effectively reduced, and the adverse effect in large-scale and continuous conventional experiments can be decreased as much as possible. Furthermore, this method provides a quantitative study of hydraulic connectivity, which is highly suited to investigate the karst groundwater table sequence with an obvious fluctuation trend.

Possible future research based on this study include the following: (i) The average karst groundwater table is calculated in a 15-day cycle in this study because of the limitations of the data itself. Future studies can attempt to calculate the average karst groundwater table in different cycles based on the feature of research objects and of data itself. (ii) The research objects (Western Jinan and Jinan spring groups) in this study are only a typical case to introduce the quantized evaluation index WTFRD; future studies can increase the number of observation wells and enlarge the range of research area. (iii) The improved grey amplitude relation can be as a pre-study method before conducting the conventional experiments, and this combined method can achieve their full potential in future. (iv) The karst groundwater table is used to calculate the WTFRD in this study, and further research can use water quality indicators such as electrical conductivity to calculate the WTFRD. (v) The grey amplitude relation model can be used to study the hysteretic nature between two variables, and it has been successfully applied in China's economic field [66]. This approach provides an idea to investigate the hysteretic time of karst groundwater movement, which deserves further study by the authors.

6. Conclusions

The potential of improved grey amplitude relation method for exploring the preferential sites of conventional experiments was researched in this study. The study areas were Western Jinan and Jinan spring groups. Taking the karst groundwater table data of Western Jinan and Jinan spring groups from 2014 to 2017 as a case, first, the average karst groundwater table was calculated using a 15-day cycle, and time series values were then obtained. Second, the WTFRD in an entire year was calculated by using these time series values. Third, to deeply analyze the hydraulic connectivity, the time series values by month were divided into different periods based on the conditions of rainfall and karst groundwater's recharge and exploitation in Jinan to calculate WTFRD. Through the above steps, the external factors with a considerable influence on WTFRD were excluded. Then, we attempted to explore the hydraulic connectivity under the smallest external disturbance conditions. The total WTFRD between Western Jinan and Jinan spring groups was 0.854 under the condition of minimal external distractions, and this value belongs to the high relation degree grade. This result indicated that there was a high hydraulic connectivity between Western Jinan and Jinan spring groups from the view of statistics. Meanwhile, the fluctuation law of karst groundwater table was similar between two sites (Figure 4). Therefore, Western Jinan could be considered preferential sites for performing conventional experiments to investigate the aquifer connectivity between Western Jinan and Jinan spring groups and reveal whether these sites can be used as the optimal sites for karst groundwater recharge.

Given the original goals of this study, we presented a new quantized evaluation index, WTFRD, using the mathematical statistics theory to explore preliminarily the hydraulic connectivity of complicated karst aquifer system, and the preferential sites of conventional experiments were screened out. This method could effectively save total operating expenses and decrease adverse effect by narrowing the scope of conventional experiment sites as much as possible. In this study, we only used Jinan as a case to illustrate the potential of improved grey amplitude relation method for exploring hydraulic connectivity. On this basis, we suggest combining the improved grey amplitude relation method with the conventional experiments to form a high-efficiency and low-cost combined method. This study of Jinan serves as a reference for optimizing the layout of recharge and exploitation to alleviate the contradiction between supply and demand of water resources. We hope that this approach can provide a new idea for future research on hydraulic connectivity.

Author Contributions: This paper was composed by collaboration among all authors. W.W. and S.Q. designed this study and helped improve its progression and clarity. Z.Z. defined the mathematical construction thinking of hydraulic modeling and wrote this paper. S.L. and L.N. helped in revising the paper. Q.H. and Q.X. supported this manuscript.

Funding: This study was supported by Shandong Provincial Key Research and Development Project (2017GSF17121) and the Danish Development Agency (DANIDA) coordinated by the DANIDA Fellowship Center (DFC) through the grant No. 17-M08-GEU.

Acknowledgments: The authors would like to acknowledge the editor and two anonymous reviewers for their valuable comments, which have greatly improved this paper.

Conflicts of Interest: The authors declare no conflict of interest.

References

1. Weyhenmeyer, C.E.; Burns, S.J.; Waber, H.N.; Macumber, P.G.; Matter, A. Isotope study of moisture sources, recharge areas, and groundwater flow paths within the eastern Batinah coastal plain, Sultanate of Oman. *Water Resour. Res.* **2002**, *38*, 2-1–2-22. [CrossRef]
2. Nakaya, S.; Uesugi, K.; Motodate, Y.; Ohmiya, I.; Komiya, H.; Masuda, H.; Kusakabe, M. Spatial separation of groundwater flow paths from a multi-flow system by a simple mixing model using stable isotopes of oxygen and hydrogen as natural tracers. *Water Resour. Res.* **2007**, *43*, 252–258. [CrossRef]
3. Fiorillo, F. Tank-reservoir drainage as a simulation of the recession limb of karst spring hydrographs. *Hydrogeol. J.* **2011**, *19*, 1009–1019. [CrossRef]
4. Malík, P.; Vojtková, S. Use of recession-curve analysis for estimation of karstification degree and its application in assessing overflow/underflow conditions in closely spaced karstic springs. *Environ. Earth Sci.* **2012**, *65*, 2245–2257. [CrossRef]
5. Uliana, M.; Banner, J.; Sharp, J. Regional groundwater flow paths in Trans-Pecos, Texas inferred from oxygen, hydrogen, and strontium isotopes. *J. Hydrol.* **2007**, *334*, 334–346. [CrossRef]
6. Raiber, M.; Webb, J.A.; Bennetts, D.A. Strontium isotopes as tracers to delineate aquifer interactions and the influence of rainfall in the basalt plains of southeastern Australia. *J. Hydrol.* **2009**, *367*, 188–199. [CrossRef]
7. Cartwright, I. Using groundwater geochemistry and environmental isotopes to assess the correction of 14C ages in a silicate-dominated aquifer system. *J. Hydrol.* **2010**, *382*, 174–187. [CrossRef]
8. Malik, P.; Haviarova, D.; Auxt, A.; Grolmusova, Z.; Michalko, J. Isotopic Composition of Waters in the Dem?novská dolina Valley and Its Underground Hydrologic System During Winter and Spring of 2010/2011. *J. Groundw. Sci. Eng.* **2013**, *1*, 14–23.
9. Varnier, C.; Hirata, R.; Aravena, R. Examining nitrogen dynamics in the unsaturated zone under an inactive cesspit using chemical tracers and environmental isotopes. *Appl. Geochem.* **2017**, *78*, 129–138. [CrossRef]
10. Kattan, Z. Using hydrochemistry and environmental isotopes in the assessment of groundwater quality in the Euphrates alluvial aquifer, Syria. *Environ. Earth Sci.* **2018**, *77*, 45. [CrossRef]
11. Li, P.; Wu, J.; Tian, R.; He, S.; He, X.; Xue, C.; Zhang, K. Geochemistry, Hydraulic Connectivity and Quality Appraisal of Multilayered Groundwater in the Hongdunzi Coal Mine, Northwest China. *Mine Water Environ.* **2018**, *37*, 222–237. [CrossRef]
12. Merritt, M.L.; Konikow, L.F. *Documentation of a Computer Program to Simulate Lake-Aquifer Interaction Using the MODFLOW Ground-Water Flow Model and the MOC3D Solute-Transport Model*; US Department of the Interior, US Geological Survey: Reston, VA, USA, 2000.
13. Froukh, L.J. Groundwater Modelling in Aquifers with highly Karstic and Heterogeneous Characteristics (KHC) in Palestine. *Water Resour. Manag.* **2002**, *16*, 369–379. [CrossRef]
14. Twarakavi, N.K.C.; Simunek, J.; Seo, S. Evaluating Interactions between Groundwater and Vadose Zone Using the HYDRUS-Based Flow Package for MODFLOW. *Vadose Zone J.* **2008**, *7*, 757–768. [CrossRef]
15. Fiorillo, F.; Pagnozzi, M.; Ventafridda, G. A model to simulate recharge processes of karst massifs. *Hydrol. Process.* **2015**, *29*, 2301–2314. [CrossRef]
16. Dafny, E.; Burg, A.; Gvirtzman, H. Effects of Karst and geological structure on groundwater flow: The case of Yarqon-Taninim Aquifer, Israel. *J. Hydrol.* **2010**, *389*, 260–275. [CrossRef]
17. Raiber, M.; White, P.A.; Daughney, C.J.; Tschritter, C.; Davidson, P.; Bainbridge, S.E. Three-dimensional geological modelling and multivariate statistical analysis of water chemistry data to analyse and visualise aquifer structure and groundwater composition in the Wairau Plain, Marlborough District, New Zealand. *J. Hydrol.* **2012**, *436–437*, 13–34. [CrossRef]

18. Qadir, A.; Ahmad, Z.; Khan, T.; Zafar, M.; Qadir, A.; Murata, M. A spatio-temporal three-dimensional conceptualization and simulation of Dera Ismail Khan alluvial aquifer in visual MODFLOW: A case study from Pakistan. *Arab. J. Geosci.* **2016**, *9*, 149. [CrossRef]
19. Maloszewski, P.; Zuber, A. Principles and practice of calibration and validation of mathematical models for the interpretation of environmental tracer data in aquifers. *Adv. Water Resour.* **1992**, *15*, 173–190. [CrossRef]
20. Chen, Z. Estimate of recharge from radiocarbon dating of groundwater and numerical flow and transport modeling. *Water Resour. Res.* **2000**, *36*, 2607–2620.
21. Perrin, J.; Jeannin, P.Y.; Zwahlen, F. Epikarst storage in a karst aquifer: A conceptual model based on isotopic data, Milandre test site, Switzerland. *J. Hydrol.* **2003**, *279*, 106–124. [CrossRef]
22. Burnett, W.C.; Aggarwal, P.K.; Aureli, A.; Bokuniewicz, H.; Cable, J.E.; Charette, M.A.; Kontar, E.; Krupa, S.; Kulkarni, K.M.; Loveless, A. Quantifying submarine groundwater discharge in the coastal zone via multiple methods. *Sci. Total Environ.* **2006**, *367*, 498–543. [CrossRef] [PubMed]
23. Lopez, O.M.; Jadoon, K.Z.; Missimer, T.M. Method of Relating Grain Size Distribution to Hydraulic Conductivity in Dune Sands to Assist in Assessing Managed Aquifer Recharge Projects: Wadi Khulays Dune Field, Western Saudi Arabia. *Water* **2015**, *7*, 6411–6426. [CrossRef]
24. Böhlke, J.K.; Smith, R.L.; Miller, D.N. Ammonium transport and reaction in contaminated groundwater: Application of isotope tracers and isotope fractionation studies. *Water Resour. Res.* **2006**, *42*, W05411. [CrossRef]
25. Edwards, T.W.D.; Birks, S.J.; St Amour, N.A.; Buhay, W.M.; Mceachern, P.; Wolfe, B.B.; Peters, D.L. Progress in isotope tracer hydrology in Canada. *Hydrol. Process.* **2005**, *19*, 303–327.
26. Carucci, V.; Petitta, M.; Aravena, R. Interaction between shallow and deep aquifers in the Tivoli Plain (Central Italy) enhanced by groundwater extraction: A multi-isotope approach and geochemical modeling. *Appl. Geochem.* **2012**, *27*, 266–280. [CrossRef]
27. Raiber, M.; Webb, J.A.; Cendón, D.I.; White, P.A.; Jacobsen, G.E. Environmental isotopes meet 3D geological modelling: Conceptualising recharge and structurally-controlled aquifer connectivity in the basalt plains of south-western Victoria, Australia. *J. Hydrol.* **2015**, *527*, 262–280. [CrossRef]
28. Martinez, J.L.; Raiber, M.; Cendón, D.I. Using 3D geological modelling and geochemical mixing models to characterise alluvial aquifer recharge sources in the upper Condamine River catchment, Queensland, Australia. *Sci. Total Environ.* **2017**, *574*, 1–18. [CrossRef] [PubMed]
29. Fiorillo, F.; Esposito, L.; Testa, G.; Ciarcia, S.; Pagnozzi, M. The Upwelling Water Flux Feeding Springs: Hydrogeological and Hydraulic Features. *Water* **2018**, *10*, 501. [CrossRef]
30. Healy, R.W.; Cook, P.G. Using groundwater levels to estimate recharge. *Hydrogeol. J.* **2002**, *10*, 91–109. [CrossRef]
31. Brodie, R.S.; Hostetler, S.; Slatter, E. Comparison of daily percentiles of streamflow and rainfall to investigate stream–aquifer connectivity. *J. Hydrol.* **2008**, *349*, 56–67. [CrossRef]
32. Copty, N.K.; Trinchero, P.; Sanchez-Vila, X.; Sarioglu, M.S.; Findikakis, A.N. Influence of heterogeneity on the interpretation of pumping test data in leaky aquifers. *Water Resour. Res.* **2008**, *44*, W11419. [CrossRef]
33. Liang, X.; Zhang, Y.K. A new analytical method for groundwater recharge and discharge estimation. *J. Hydrol.* **2012**, *450–451*, 17–24. [CrossRef]
34. Heße, F.; Savoy, H.; OsorioMurillo, C.A.; Sege, J.; Attinger, S.; Rubin, Y. Characterizing the impact of roughness and connectivity features of aquifer conductivity using Bayesian inversion. *J. Hydrol.* **2015**, *531*, 73–87. [CrossRef]
35. Qian, J.; Wang, L.; Ma, L.; Lu, Y.H.; Zhao, W.; Zhang, Y. Multivariate statistical analysis of water chemistry in evaluating groundwater geochemical evolution and aquifer connectivity near a large coal mine, Anhui, China. *Environ. Earth Sci.* **2016**, *75*, 747. [CrossRef]
36. Panagopoulos, G.P.; Angelopoulou, D.; Tzirtzilakis, E.E.; Giannoulopoulos, P. The contribution of cluster and discriminant analysis to the classification of complex aquifer systems. *Environ. Monit. Assess.* **2016**, *188*, 591. [CrossRef] [PubMed]
37. Owen, D.D.R.; Pawlowsky-Glahn, V.; Egozcue, J.J.; Buccianti, A.; Bradd, J.M. Compositional data analysis as a robust tool to delineate hydrochemical facies within and between gas-bearing aquifers. *Water Resour. Res.* **2016**, *52*, 5771–5793. [CrossRef]

38. King, A.C.; Raiber, M.; Cox, M.E.; Cendón, D.I. Comparison of groundwater recharge estimation techniques in an alluvial aquifer system with an intermittent/ephemeral stream (Queensland, Australia). *Hydrogeol. J.* **2017**, *25*, 1759–1777. [CrossRef]
39. Wu, S.; Liu, S.; Li, M. Study of Integrate Models of Rough Sets and Grey Systems. In *Fuzzy Systems and Knowledge Discovery*; Lecture Notes in Computer Science; Springer: Berlin/Heidelberg, Germany, 2005; pp. 1313–1323.
40. Yang, Y.; Forrest, J.; Liu, S. A brief introduction to grey systems theory. *Grey Syst. Theory Appl.* **2012**, *2*, 89–104.
41. Liu, S.; Forrest, J.; Vallee, R. Emergence and development of grey systems theory. *J. Zhejiang Wanli Univ.* **2003**, *38*, 1246–1256. [CrossRef]
42. Deng, J.L. The main method of the intrinsic gray system. *J. Syst. Eng. Theory Pract.* **1986**, *6*, 60–65.
43. Zhu, J. Aapplication of grey clustering method in evaluating environment-economic benefit of enterprise. *Rural Eco-Environ.* **1991**, *7*, 39–41.
44. Feng, J.; Yi, L.; Liu, X. Grey Correlation Analysis of Main Pollutants in Waters of Baiyangdian Lake. *J. Eng. Sci.* **1995**, 42–43.
45. Dang, Y.; Liu, S.; Liu, B.; Mi, C. Improvement on Degree of Grey Slope Incidence. *Eng. Sci.* **2004**, *6*, 41–44.
46. Yu, G.Q.; Li, Z.B.; Zhang, X.; Li, P.; Du, Z. BP artificial neural network model of groundwater dynamic and analysis on the improved grey slope coefficient correlation degree. *J. Xian Univ. Archit. Technol.* **2009**, *4*, 566–570.
47. Liu, H. The impact of human behavior on ecological threshold: Positive or negative?—Grey relational analysis of ecological footprint, energy consumption and environmental protection. *Energy Policy* **2013**, *56*, 711–719.
48. Yin, K.; Xu, Y.; Li, X.; Jin, X. Sectoral Relationship Analysis on China's marine-land economy based on a novel grey periodic relational model. *J. Clean. Prod.* **2018**, *197*, 815–826. [CrossRef]
49. Shi, H.; Liu, S.; Fang, Z.; Cheng, Y.; Zhang, H. The model of grey periodic incidence and their rehabilitation. In Proceedings of the 2007 IEEE International Conference on Systems, Man and Cybernetics, Montreal, QC, Canada, 7–10 October 2007; pp. 2219–2222.
50. Shi, H.X.; Liu, S.F.; Fang, Z.G.; Yang, B.H. Grey amplitude incidence model. *Syst. Eng. Theory Pract.* **2010**, *30*, 1828–1833.
51. Ran, J.; Zhao, R. Rotor Fault Mode Identification Based on Grey Correlation Degree of Frequency Domain Amplitude. *J. Vib.* **2013**, 1019–1096.
52. Zhang, Z.; Liu, Y.; Zhang, F.; Zhang, L. Study on dynamic relationship of spring water in Jinan spring area based on gray relational analysis. *IOP Conf. Ser. Earth Environ. Sci.* **2018**, *128*, 012068. [CrossRef]
53. Qian, J.; Zhan, H.; Wu, Y.; Li, F.; Wang, J. Fractured-karst spring-flow protections: A case study in Jinan, China. *Hydrogeol. J.* **2006**, *14*, 1192. [CrossRef]
54. Wang, W.; Page, D.; Zhou, Y.; Vanderzalm, J.; Dillon, P. Roof Runoff Replenishment of Groundwater in Jinan, China. *J. Hydrol. Eng.* **2015**, *20*, B5014005. [CrossRef]
55. Liu, J.; Zhu, X.; Qian, X. Study of Some Problems on the Development and Protection of Fracture-karst Water Resources in North China. *Acta Geol. Sin.* **2000**, *74*, 344–352.
56. Wang, J.; Jin, M.; Lu, G.; Zhang, D.; Kang, F.; Jia, B. Investigation of discharge-area groundwaters for recharge source characterization on different scales: The case of Jinan in northern China. *Hydrogeol. J.* **2016**, *24*, 1723–1737. [CrossRef]
57. Kang, F.; Jin, M.; Qin, P. Sustainable yield of a karst aquifer system: A case study of Jinan springs in northern China. *Hydrogeol. J.* **2011**, *19*, 851–863. [CrossRef]
58. Wang, J.; Jin, M.; Jia, B.; Kang, F. Hydrochemical characteristics and geothermometry applications of thermal groundwater in northern Jinan, Shandong, China. *Geothermics* **2015**, *57*, 185–195. [CrossRef]
59. Luo, S.; Ma, W.; Wang, X. A case study on indicator system of urban environmental protection and ecological construction. *Acta Ecol. Sin.* **2003**, *23*, 45–55.
60. Liu, Y.; Zhang, Z.; Zhang, F. Coupling Correlativity between Economic Development and Water Environment Monitoring Indicators. *J. Econ. Water Resour.* **2018**, *36*, 21–24.
61. Zhou, J.; Xing, L.T.; Teng, Z.X.; Wang, L.Y. Study on the threshold of main factors restricting Jinan large karst springs spewing. *J. East China Norm. Univ.* **2015**, *2015*, 146–156.
62. Qi, X.F.; Wang, Y.S.; Yang, L.Z.; Liu, Z.Y.; Wang, W.; Li, W.P. Time lags variance of groundwater level response to precipitation of Jinan karst spring watershed in recent 50 years. *Carsol. Sin.* **2016**, *35*, 384–393.

63. Zhang, Z.; Liu, Y.; Zhang, F. Study on groundwater resources protection in Jinan spring area based on Holt-Winters Model. *J. Earth Environ.* **2018**, *9*, 257–265.
64. Cai, W.; Gao, Z.; Wang, Q. *Research on Connections between Jinan Karst Waters*; Geologied Publishing House: Beijing, China, 2013; pp. 77–81.
65. Gao, Z.; Xu, J.; Wang, S.; Li, C.; Han, K.; Li, J.; Luo, F.; Ma, H. The distribution characteristics and hydrogeological significance of trace elements in karst water, Jinan, China. *Earth Sci. Front.* **2014**, *21*, 135–146.
66. Song, C.; Shi, H.; Qi, Y. Research on the rule of vehicle traffic accidents based on gray correlation analysis. *China Saf. Sci. J.* **2010**, *20*, 40–43.